Energy behavior on side structure in event of ship collision subjected to external parameters

Aditya Rio Prabowo [a,b,*]**, Dong Myung Bae** [c]**, Jung Min Sohn** [c]**, Bo Cao** [d]

[a] *Interdiscliniary Program of Marine Convergence Design, Pukyong National University, Republic of Korea*

[b] *Department of Naval Architecture, Diponegoro University, Republic of Indonesia*

[c] *Department of Naval Architecture and Marine Systems Engineering, Pukyong National University, Republic of Korea*

[d] *China Shipbuilding Industry Corporation Economic Research Center, People's Republic of China*

*Corresponding author.

E-mail address: aditya@pukyong.ac.kr (A.R. Prabowo).

Abstract

The safety of ships in regards to collisions and groundings, as well as the navigational and structural aspects of ships, has been improved and developed up to this day by technical, administrative and nautical parties. The damage resulting from collisions could be reduced through several techniques such as designing appropriate hull structures, ensuring tightness of cargo tanks as well as observation and review on structural behaviors, whilst accounting for all involved parameters. The position during a collision can be influenced by the collisions' location and angle as these parts are included in the external dynamics of ship collisions. In this paper, the results of several collision analyses using the finite element method were used and reviewed regarding the effect of location and angle on energy characteristic. Firstly, the capabilities of the structure and its ability to resist destruction in a collision process were presented and comparisons were made to other collision cases. Three types of collisions were identified based on the relative location of contact points to each other. From the results, it was found that the estimation of internal energy by the damaged ships differed in range from 12%–24%. In the second stage, the results showed that a collision between 30 to 60 degrees produced higher level energy than a collision in the perpendicular position.

Furthermore, it was concluded that striking and struck objects in collision contributed to energy and damage shape.

Keywords: Engineering, Structural engineering

1. Introduction

Since the development of transportation began, the collision phenomenon has become a remarkable phenomenon both on the sea and on the land. Limitless possibilities of both scenarios and their causes resulted in the fact that makes the investigation and research in this field was conducted continuously until the 20th century. The tragic accident of the Royal Merchant Ship Titanic on the Atlantic Ocean in 1912 is a well-known example of this phenomenon for water transportation modes. This accident led related parties to perform investigation and research to make rules and safety codes for the sea in order to avoid the same tragedy in the future. The phenomenon process in ship collision is basically divided into two main parts, i.e.: external dynamics and internal mechanics of ship collision which are both interconnected to each other. Methods to assess this phenomenon have continued to improve up to this day. The assessment method is classified into four-known-types (Zhang, 1999). In order to achieve a satisfactory result in collision analysis, Kitamura from Japan stated in his previous work (Kitamura, 2001) that the analysis should be based on real accidents (Bae et al., 2016), experiments, or the finite element method/FEM approach (Prabowo et al., 2016; Zakki et al., 2016). Previous works on impact phenomenon were performed in the field of collision between structures by Haris and Amdahl (2013), the interaction between ice and structures by Cao (2016), grounding analysis by AbuBakar and Dow (2013), and statistical data on ship collisions by Pedersen and Zhang (1999). These works were performed using FEM approach and real collision data. The FEM implementation is preferred these days as the rapid growth of computational instrument. Numerical data can present reliable results if phenomenon model is defined properly.

In this present work, authors wanted to present a study on ship collision phenomenon using the finite element method which focused on the internal energy and damage extent on a structure after several collision scenarios were deployed. The scenarios were made based on different locations and angles of collisions in relation to the position of both involved ships.

2. Theory

Defining the parameter on the external dynamic during a collision process between two objects is performed in some scenarios in order to make predictions through research, or even by predicting the scenario for the re-construction phenomena from real accidents which have already taken place. This principle is also used in

re-constructing, making and analyzing scenarios of ship collisions. In 1982, Petersen studied a procedure for time simulation of the outer dynamic in ship collisions. The hydrodynamic forces acting on the ship's hull during the collision were calculated by a ship theory. The involved ships were essentially treated as rigid bodies with all deformations taking place in the contact area. The structural responses in the contact area were modelled as non-linear springs (Petersen, 1982).

The external dynamics of ship collisions have the role as the action in the collision process. According to Newton's Third Law about force, for every action, there is an equal and opposite reaction. The statement means that in every interaction, there is a pair of forces acting on the two interacting objects. The size of the force on the first object equals the size of the force on the second object. When the external dynamic causes the action in the collision process, the reaction as the result of the action on a ships structure will be called the internal mechanics of ship collision.

3. Materials

In order to obtain the most similar material properties of real ship materials, hardness and chemical composition tests were conducted. These tests were performed by using material samples from the side shell of a struck ship in a previous accident at Sunda strait. Hardness tests were performed using test method ASTM E18-05 with test type Rockwell Hardness Number A (HRA) and load test 60 kgf (ASTM International, 2006). As for chemical composition, the test was conducted using WAS/PMI-MASTER Pro spectrometer from Oxford Instruments. The results and comparisons with the predicted material of both tests are presented in Table 1 and Table 2. After comparing the results from testing with theory and other material characteristics from the literature review (Callister, 2007), it could be concluded that the sample of the struck ship material was included in plain medium carbon steel, type AISI 1030 specifically. The difference of sulfur composition could be affected by the treatment of the ship hull during previous repair activity. However, other compositions had good correlation regarding similarities between ship material and AISI 1030.

Table 1. Conclusions of hardness tests.

Test Mode	Hardness	
	Ship Material	Reference (1030)
Hardness Rockwell Number A	50.37	–
Hardness Rockwell Number B	81.49	80
Hardness Vickers	154.35	155

Table 2. Results of chemical composition tests.

Element	Composition (%)	
	Specimen	**Composition of 1030**
Iron (Fe)	98.600	98.67–99.13
Manganese (Mn)	0.848	0.60–0.90
Carbon (C)	0.290	0.27–0.34
Phosphorous (P)	0.034	≤0.04
Sulfur (S)	0.095	≤0.05

$$\sigma_y = \left[1 + \left(\frac{\varepsilon}{C}\right)^{\frac{1}{P}}\right]\left(\sigma_0 + \beta E_P \varepsilon_P^{eff}\right) \tag{1}$$

$$E_P = \frac{E_{\tan}E}{E - E_{\tan}} \tag{2}$$

where σ_y is yield stress, σ_0 is initial yield stress, ε_p^{eff} is effective plastic strain, *C-P* are Cowper-Symonds strain rate parameters, β is hardening parameter, E_p is plastic hardening modulus, and $E_{\tan}$ is tangent modulus, and E is Young's modulus.

Plastic-kinematics material is considered in the numerical analysis and summarized in Table 3. The yield function of plastic-kinematics material is given as Eq. (1) and Eq. (2). Isotropic and kinematic contributions may be varied by adjusting the hardening parameter. Zero value of the hardening characteristic implies that only kinematic hardening is applied. The strain rate is accounted for using the Cowper-Symonds model which consists of two parameters. Experiment results of Amdahl and Kavlie (1992) indicated that the ductility of mild steel is in the range of 0.20–0.35. As an additional consideration of Ozguc et al. (2005), the failure strain 0.2 is implemented into the present virtual experiment.

Table 3. Material model for virtual experiment.

Properties	Value
Density (kg/m^3)	7850
Young's modulus (MPa)	210000
Poisson's ratio	0.30
Yield stress (MPa)	440
Hardening parameter	0
Strain rate parameter − *C* (/s)	3200
Strain rate parameter − *P*	5
Failure strain	0.20

4. Instrumentation

Numerical simulations of the collisions were conducted with the LS-DYNA explicit code. The element of choice was the one point quadrature Belytschko − Tsay element, which was both accurate and effective. The Belytschko − Tsay (BT) shell element as a computationally efficient has become the default shell element formulation. Since the BT shell element is based on perfectly flat geometry, warpage is not considered. The effect of neglecting warpage may lead to less than accurate results, but later is difficult to verify in practice. The mesh size must be large enough to obtain a practical simulation time, but sufficiently small to capture the major deformation modes. Alsos and Amdahl (Alsos and Amdahl, 2007) suggested that the element-length-to-thickness ratio should be within the range of 5–10 so that the local stress and strain fields could be captured well. The mesh in the core area has an element − length − to − thickness ratio of approximately 8–10.

4.1. Design and model

A 144 m cargo reefer would be used as the striking ship with rigid body characteristic was implemented on its structures. Furthermore, a Ro-Ro passenger ship with a length of 85 m was used as the deformable struck ship. The main dimension from both of the ships is presented on Table 4 and Table 5. The models from the striking and the struck ship are presented in Fig. 1.

4.2. Methodology

The location of the target point was determined on the side hull of the fore end region exactly between the middle deck and the main deck. In the present work, three collision cases were conducted and simulated using finite element analysis in terms of location. They were denoted as Target I, in which the striking ship collides with the side shell near the location of the middle deck at approximately 9 m from the baseline; Target II in which the striking ship collides with the side shell between the middle deck and the erection deck at 10 m from the base line; and Target III in which the striking ship collides with the side shell between Scenario II

Table 4. Main dimension of striking ship.

Type of ship		Cargo reefer
Length over all (m)	L_{oa}	144.50
Breadth moulded (m)	B	19.80
Design draft (m)	T	5.60
Depth (m)	H	10.20

Table 5. Dimension and structural data of struck ship.

Type of ship		Ro-Ro passenger
Length over all (m)	L_{oa}	85.92
Length between perpendicular (m)	L_{pp}	78.00
Breadth moulded (m)	B	15.00
Design draft (m)	T	4.30
Depth (m)	H	10.40
Frame spacing (mm)	a	600
Width between outer and inner shell (m)	w	3.50

and the erection deck at 11 m from the keel. The striking ship is given a velocity of 6.17 m/s to move to the designated target point on the deformable structure of the struck ship. Time simulation in the present virtual experiment is 0.567 s.

Besides location, the collision angle based on the position of the two ships during the collision was also taken into account. Five different collision angles were used in the simulation, including 30°, 60°, 90°, 120°, and 150°. Illustrations for proposed target locations and collision angles are given in Fig. 2 and Fig. 3, consecutively. The internal energy and crushing load were observed as dependent variables to obtain the characteristics of the effects of collisions locations and angles in the event of a ship-ship collision.

5. Results and discussion

5.1. Target point location

The internal energy in collision analysis was identified as the energy that was needed to plastically deform or even destroy the structure of a struck ship when a collision occurred. Fig. 4 presented the internal energy of collision simulation. The differences in the graph represented the difference of capabilities between parts of the ship structure when resisting a striking ship.

At the deepest penetration, Scenario III had the smallest energy compared to the other two scenarios. The differences of internal energy between all scenarios were in the range of 12%–24%. Internal energy from Scenario II was found to be bigger than Scenario I with 12.19%, and 24.39% bigger than Scenario III at the end of penetration. The difference between Scenario I and Scenario III was 13.89%. Other related responses were connected to the contact force. This response was defined as a force that acted at the point of contact between two objects, in the opposite direction of body forces. Fig. 5 presents the contact force for three scenarios based on location.
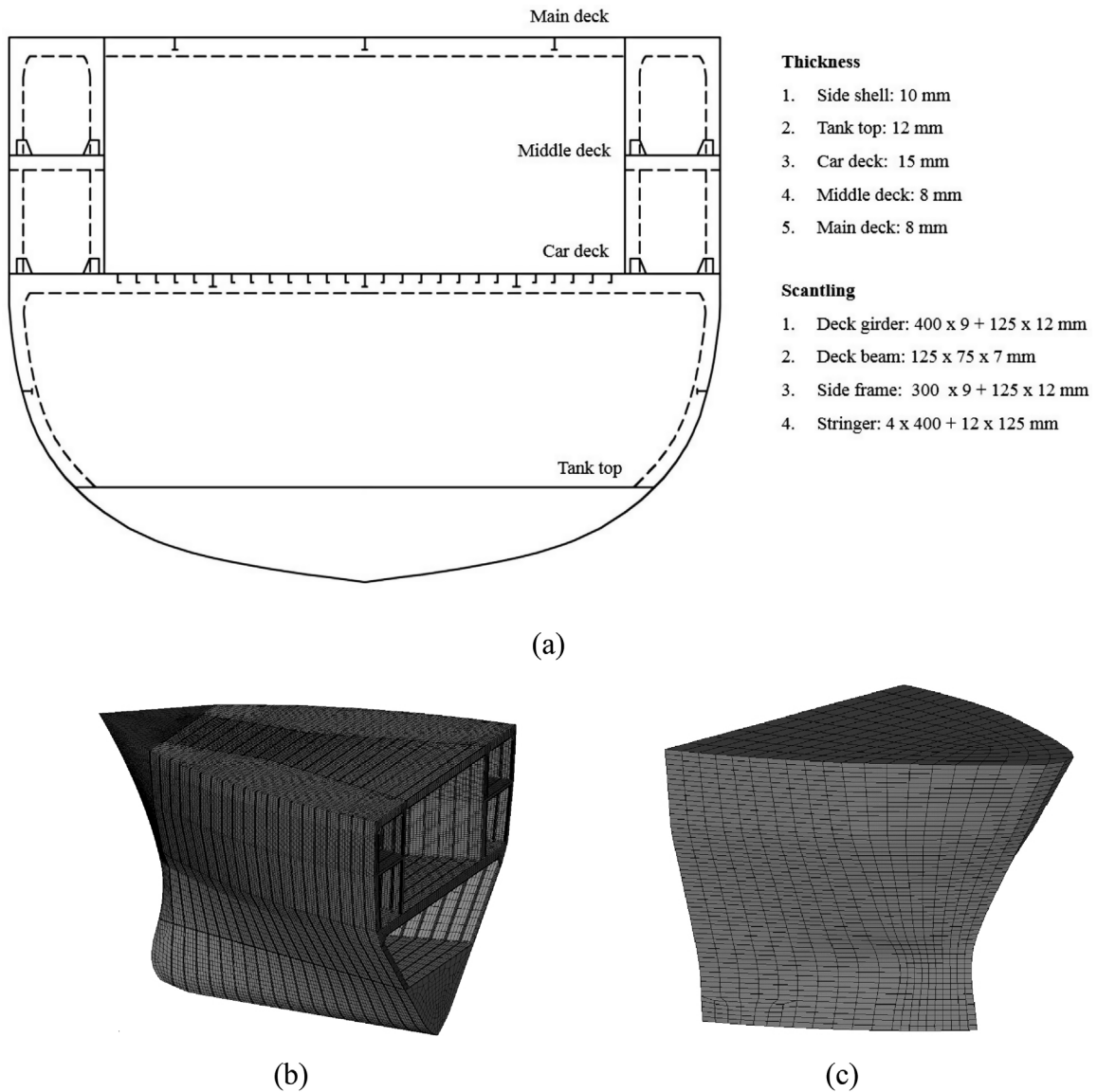
Thickness

1. Side shell: 10 mm
2. Tank top: 12 mm
3. Car deck: 15 mm
4. Middle deck: 8 mm
5. Main deck: 8 mm

Scantling

1. Deck girder: 400 x 9 + 125 x 12 mm
2. Deck beam: 125 x 75 x 7 mm
3. Side frame: 300 x 9 + 125 x 12 mm
4. Stringer: 4 x 400 + 12 x 125 mm

(a)

(b)

(c)

Fig. 1. Geometry models for collision analysis: (a) midship section of struck ship, (b) struck ship, and (c) striking ship.

Fluctuation on the force-penetration curve (Fig. 5) indicated a process of material destruction per depth of penetration. The peak of fluctuation likely occurred during initial tearing, and when destruction on the structural member had already begun. The collision in Scenario I reached the highest force at the deepest penetration compared to the other scenarios where the contact location of the scenario was near the middle deck, and the side shell which was strengthened by a transverse frame and was also reinforced by the longitudinal deck. The contact force for Scenario III where the collision happened near the erection deck was smaller than the other scenarios. It indicated that the structure in the area of Scenario III was not as strong
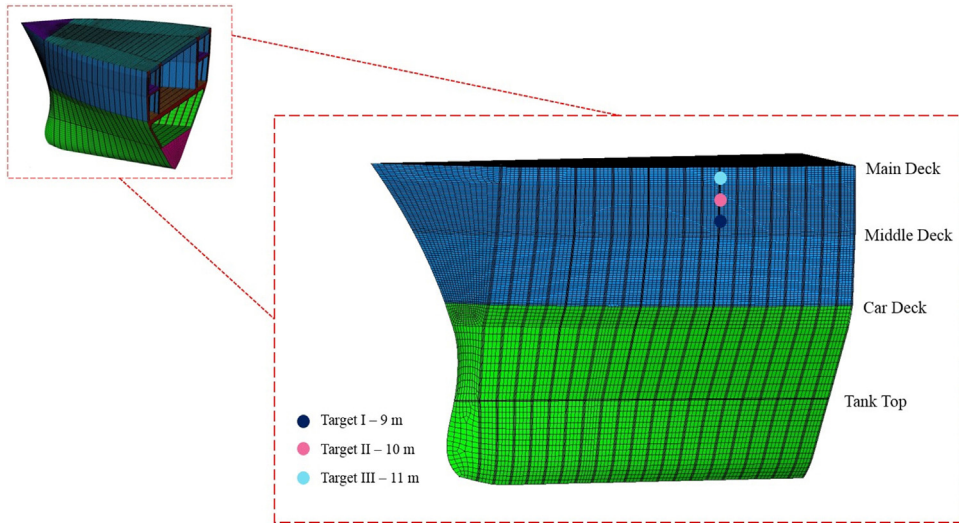
Fig. 2. Proposed location for target point in collision analysis.

as the structure in other locations. Differences in terms of the contact force between Scenario II and Scenario I and III were 6.86% and 21.15% consecutively.

5.2. Collision angle

This section contains the results from several simulations, as well as a discussion of five cases based on collision angle parameters. The results of collision simulation such as internal energy and crushing load are presented together with damage and stress distribution after the collision process. There are many possible scenarios in
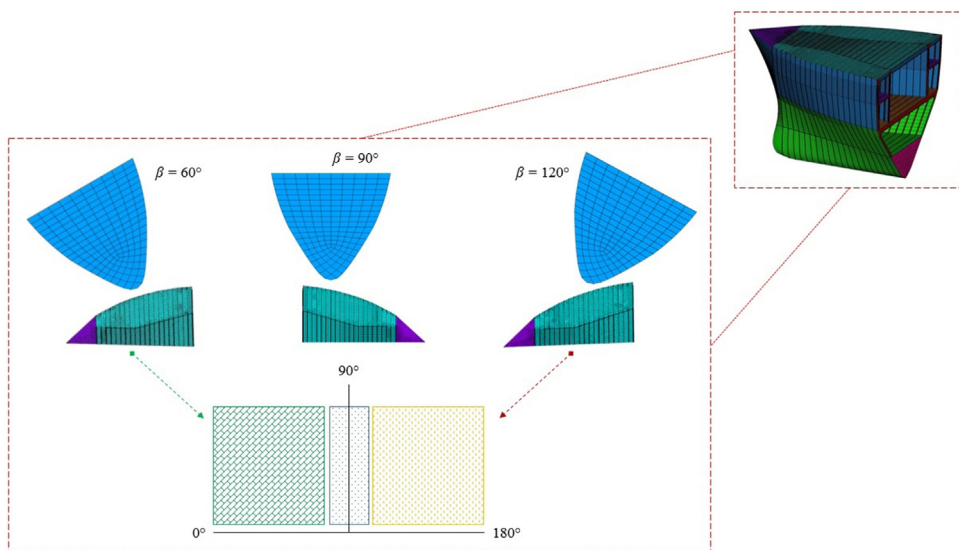
Fig. 3. Position of collision angle on side collision process.
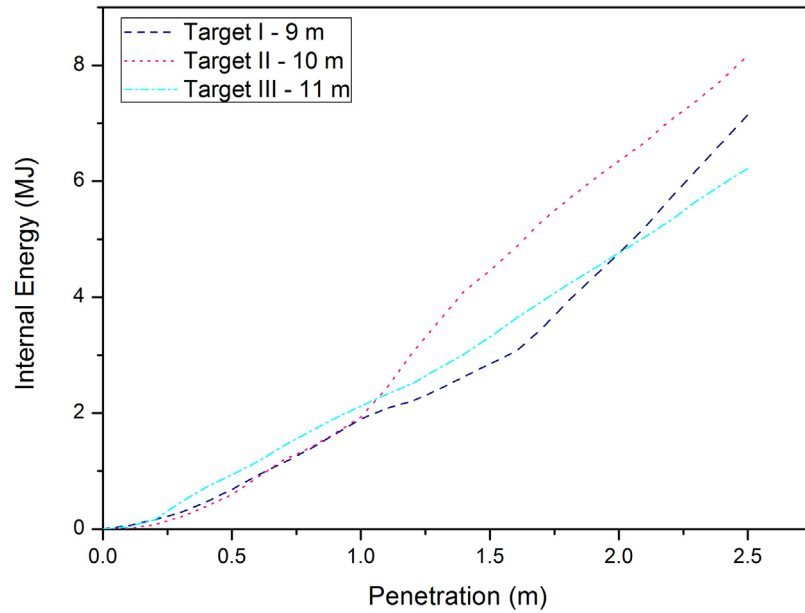
Fig. 4. Internal energy versus penetration curves for all targets.

ship collision accidents which a study regarding characteristic of collision scenario is needed. One of the notable characteristics in collision scenarios is the collision angle between struck and striking objects, or β on external dynamic. In this study, five degrees were proposed to obtain information regarding how significant the effect was when the collision angle changed.
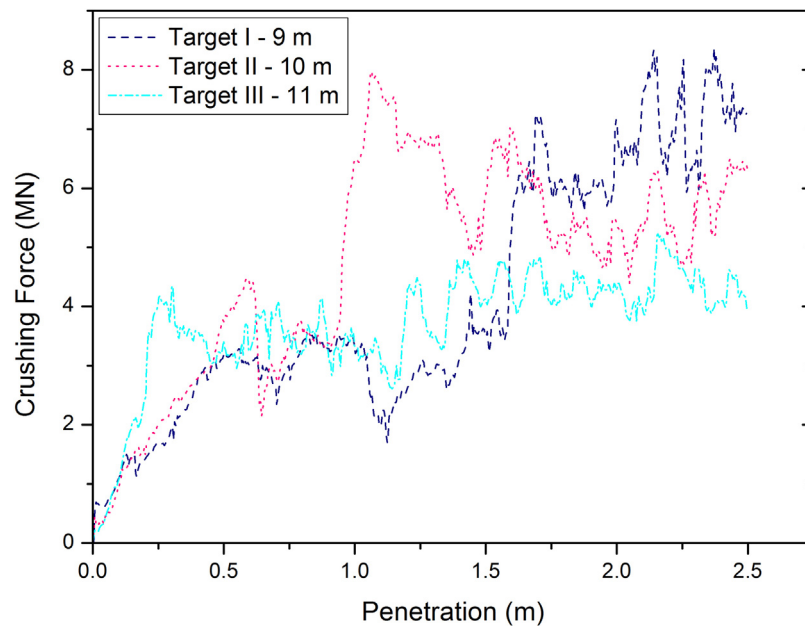
Fig. 5. History of crushing force during collision process for all locations.

(a)   (b)
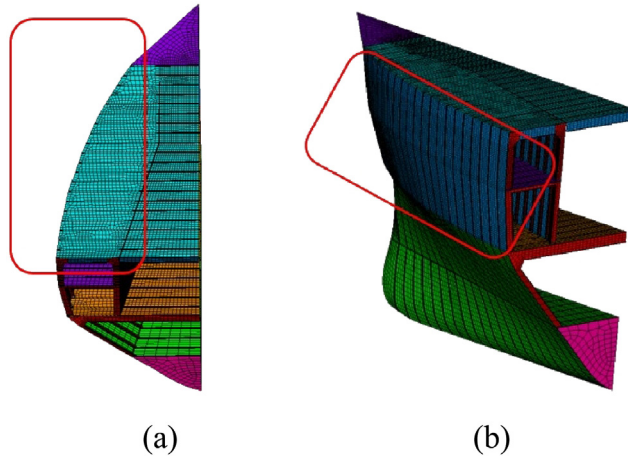
Fig. 6. Contact point section: (a) upper view, and (b) diagonal view.

When using collision angles of 30° and 60°, it was assumed that the striking ship was heading to the struck ship from a diagonal direction of the struck ship's forepeak. In the case of 120°and 150°, it was assumed that the striking ship was heading to the struck ship from a diagonal direction of the struck ship's after peak. This four degrees would be compared with a scenario where the position of the struck and striking ship was perpendicular. The location of impact point for each angle was the same but because the location of the collision was in the forepeak

Fig. 7. Energy and load for perpendicular collision.
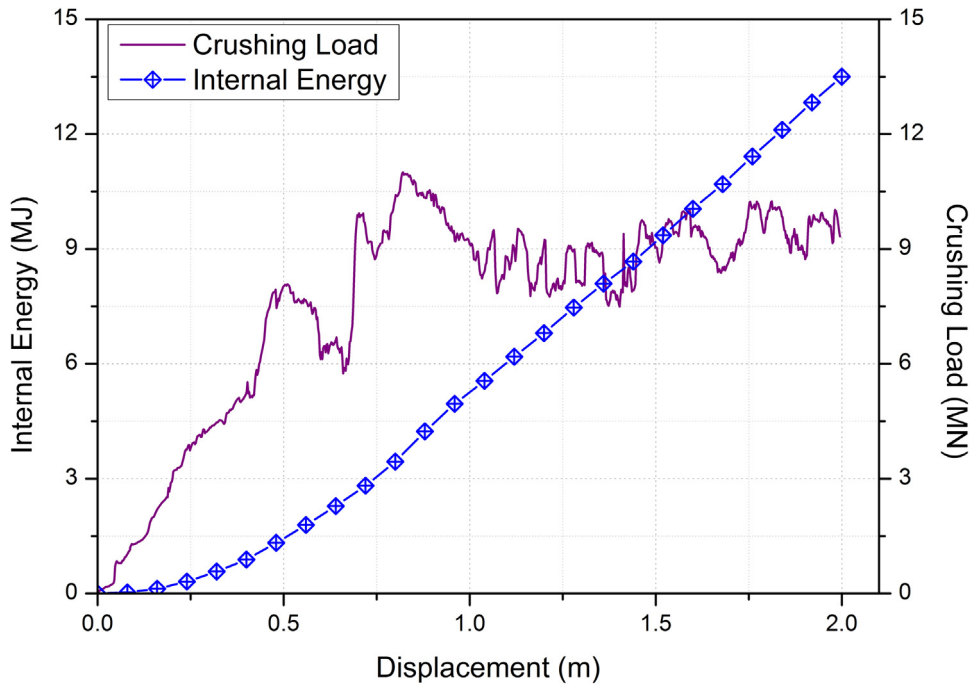
Fig. 8. Energy and load for collision with $\beta = 150°$.

area it was oval or streamline. The size and shape of contact point sections varied for each scenario with different angles. The illustration of the contact point section is presented in Fig. 6. The results of calculation indicated that collisions with a position between struck and striking ship angles below and above 90° (oblique)
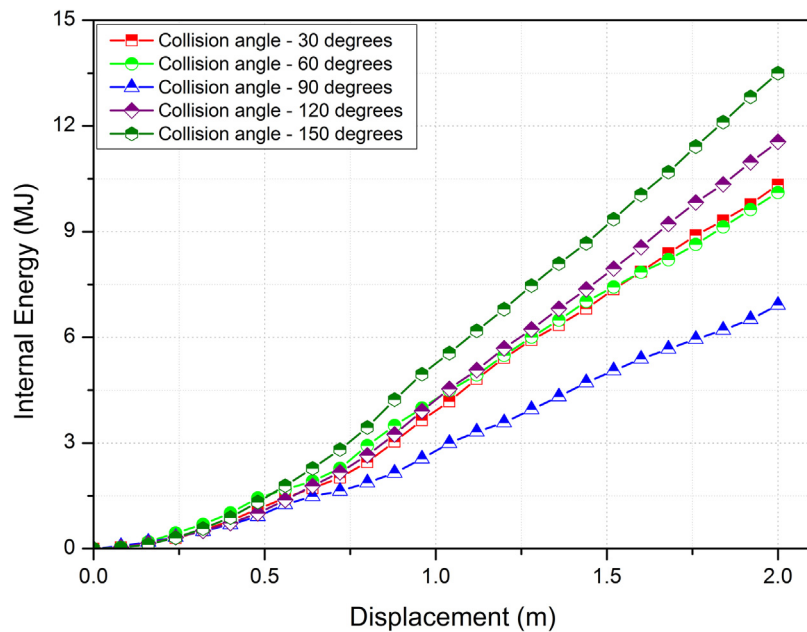

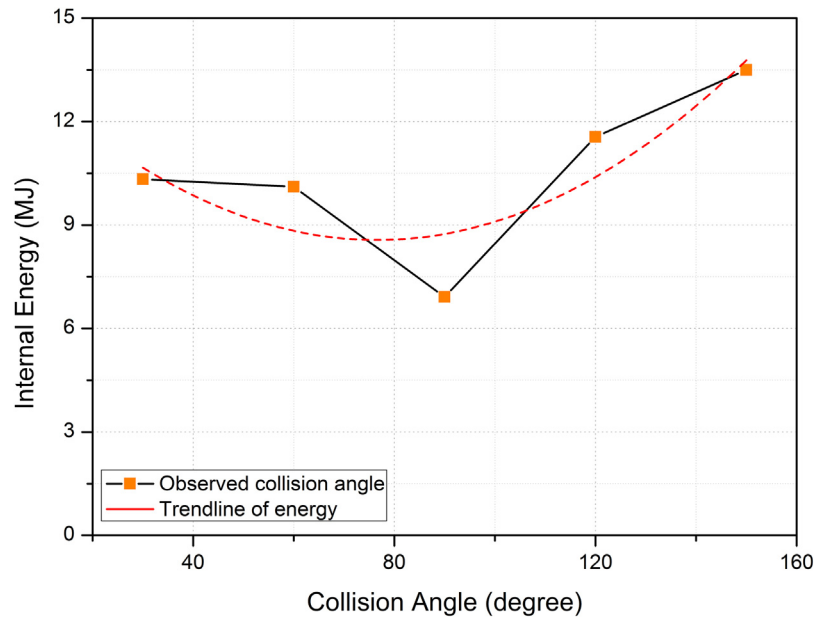**Fig. 9.** Energy behaviour as displacement of striking ship for all cases.

Fig. 10. Trend-line of energy in the end collision event.

produced bigger internal energy than collisions in the perpendicular position. In terms of internal energy, the difference between the perpendicular position (Fig. 7), and 150° (Fig. 8) was the highest with a difference of approximately more than 48%. The difference between overall simulations is in the range of 30%–50%.

These results were forming a pattern where if the collision angle was closer to 90°, the internal energy was rising but when the collision angle was right on 90°, the energy was found to be smaller. The internal energy would also decrease if the collision angle was altered to be closer to 0° and 180°. This phenomena occurred because if the collision angle tended to be closer to 0° and 180°, sliding case would
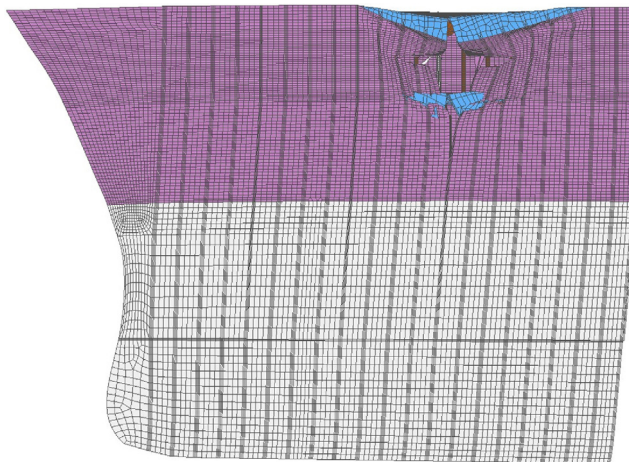

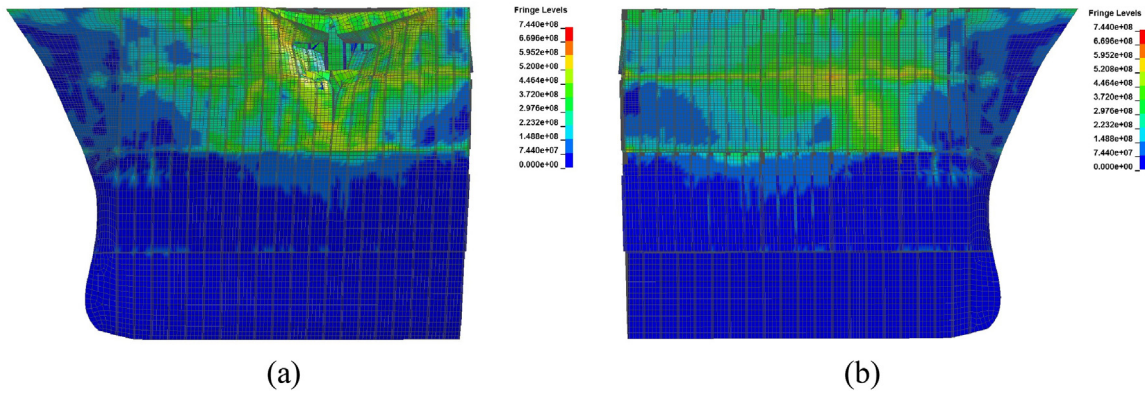**Fig. 11.** Damage pattern on collision with $\beta = 90°$.

Fig. 12. Stress distribution on side structure for β = 90°: (a) outer shell, and (b) inner shell.

take place between the struck and striking ship as they were glancing each other and less penetration would occur during the collision process. In the case of a collision angle of 90° for the same time duration, the side tip of the striking ship for 60° and 120° would have direct contract with the side hull of the struck ship earlier than 90°, so that the amount of absorbed energy was found to be bigger than 90° at the end of the collision process.

The energy pattern of all simulations as presented in Fig. 9 and Fig. 10 indicated that the energy in the collision process forming parabolic or quadratic function graph was 90° on the lowest level, and 30° as well as 150° on the highest point. The collisions which happened before and after 90° had undergone an early collision when the side of the tip from the striking bow made contact with the side shell of the struck body. However, the tip of the striking bow had no contact with the target point. This situation made more structure of side structure on the struck ship deformed and internal energy during collision process increased.
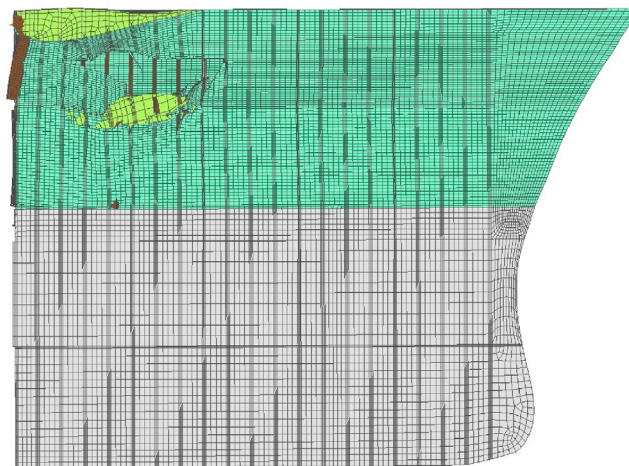

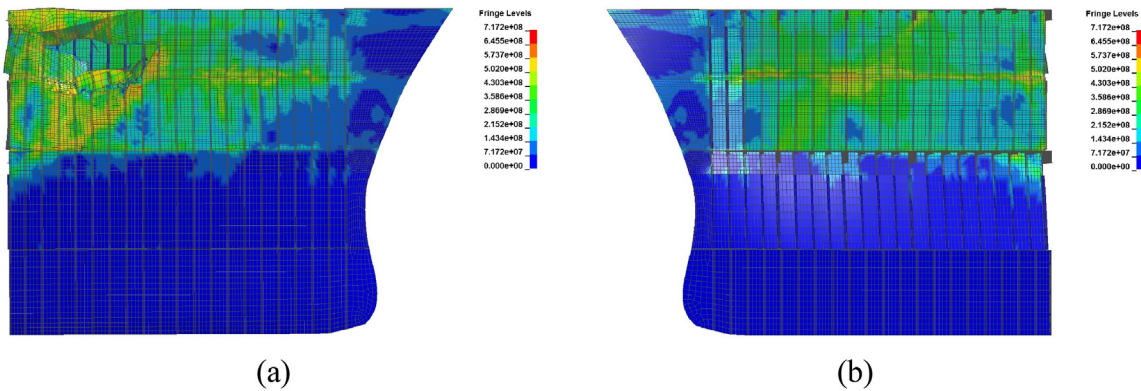**Fig. 13.** Damage pattern on collision with β = 120°.

Fig. 14. Stress distribution on side structure for $\beta = 120°$: (a) outer shell, and (b) inner shell.

In terms of stress distribution (Fig. 11, Fig. 12, Fig. 13 and Fig. 14), there were no significant differences found on either the inner or outer shell. However, during the collision with $\beta = 120°$, the maximum stress took place on certain locations on the connection between the middle deck and inner shell. This stress concentration was formed due to the displaced middle deck as a result of the collision process and the damage to the outer shell on the collision with $\beta = 60°$ was less remarkable than the collision by the angle on the opposite direction in the Cartesian coordinate system.

6. Conclusion

This paper described the study of collision phenomenon of ship-to-ship collisions, specifically on side collisions. Several collision scenarios were proposed and investigated in relation to different locations and angles. The results indicated that the collisions below and above the perpendicular position produced a higher energy. The influences of the striking bow and target point section area were predicted to give significant effects on structural responses. If the proposed target point section was determined on the parallel middle body of the ship, the energy and load were expected to have no remarkable difference. Finite element simulation is widely considered as a powerful method to predict and estimate various phenomenon, including collisions which involves high nonlinearities.

7. Related work

In order to achieve a satisfactory result during analysis and post-processing stage, the authors recommend to conduct material testing and experiments, especially for marine steel materials. Realistic results are highly influenced by material models and this kind of experiment will provide better accuracy than those constrained to the literature review. If reasonable costs in both instruments and materials can be afforded, structural-level experiments are encouraged to be conducted in model-

scale. The combination between material and structural experiments can become remarkable benchmarks for further study. Another proposed option is to conduct an investigational survey on ships involved in collision accidents. Real data of tearing patterns and damage geometry provides realistic foundations that can be used in comparative studies between real phenomenon and virtual experiments.

Declarations

Author contribution statement

Aditya Rio. Prabowo: Conceived and designed the experiments; Performed the experiments; Analyzed and interpreted the data; Contributed reagents, materials, analysis tools or data; Wrote the paper.

Dong Myung Bae, Jung Min Sohn, Bo Cao: Contributed reagents, materials, analysis tools or data.

Funding statement

Competing interest statement

The authors declare no conflict of interest.

Additional information

No additional information is available for this paper.

Acknowledgements

References

AbuBakar, A., Dow, R.S., 2013. Simulation of ship grounding damage using the finite element method. Int. J. Solids Struct. 50, 623–636.

Alsos, H.S., Amdahl, J., 2007. On the resistance of tanker bottom structures during stranding. Mar. Struct. 20, 218–237.

Amdahl, J., Kavlie, D., 1992. Experimental and Numerical Simulation of Double Hull Stranding. DNV-MIT Work Shop on Mechanics of Ship Collision and Grounding. DNV, Norway.

ASTM International, 2006. ASTM E18-15 standard test methods for rockwell hardness of metallic materials. West Conshohocken, PA, USA.

Bae, D.M., Prabowo, A.R., Cao, B., Zakki, A.F., Haryadi, G.D., 2016. Study on collision between two ships using selected parameters in collision simulation. J. Mar. Sci. Appl. 15, 63–72.

Callister Jr., W.D., 2007. Material science and engineering; an introduction, Seventh edition John Wiley & Sons (Publisher), Inc., NY, USA.

Cao, B., 2016. Study on the damage characteristic caused by collision between ship structure and level ice. Ph.D. Thesis. Department of Naval Architecture and Marine Systems Engineering, Pukyong National University, Busan, Korea.

Haris, S., Amdahl, J., 2013. Analysis of ship–ship collision damage accounting for bow and side deformation interaction. Mar. Struct. 32, 18–48.

Kitamura, O., 2001. FEM approach to the simulation of collision and grounding damage. Mar. Struct. 15, 403–428.

Ozguc, O., Das, P.K., Barltrop, N., 2005. A comparative study on the structural integrity of single and double skin bulk carriers under collision damage. Mar. Struc. 18, 511–547.

Pedersen, P.T., Zhang, S., 1999. Effect of ship structure and size on grounding and collision damage distributions. Ocean Eng. 27, 1161–1179.

Petersen, M.J., 1982. Dynamics of ship collision. Ocean Eng. 9 (4), 295–329.

Prabowo, A.R., Bae, D.M., Sohn, J.M., Zakki, A.F., 2016. Evaluating the parameter influence in the event of a ship collision based on the finite element method approach. Int. J. Technol. 4, 592–602.

Zakki, A.F., Windyandari, A., Bae, D.M., 2016. The development of new type free-fall lifeboat using fluid structure interaction analysis. J. Mar. Sci. Technol. 24, 575–580.

Zhang, S., 1999. The mechanics of ship collisions. Ph.D. Thesis. Department of Naval Architecture and Offshore Engineering, Technical University of Denmark, Lyngby, Denmark.